Supplementary Materials and Methods

Supplementary Tables 1–43

Supplementary Figures 1–26

Supplementary References

SUPPLEMENTARY MATERIALS AND METHODS

Expression and purification of PCY1 enzyme

Purification of PCY1 was adopted from the literature.[1] Overexpression of PCY1 was performed in *E. coli* BL21(DE3) grown in terrific broth media. Cultures were inoculated and grown at 30 °C until the OD_{600} reached 0.6. Cultures were cooled at 18 °C for 1 h prior to induction of protein expression by the addition of 0.3 mM isopropyl-β-d-thiogalactopyranoside (IPTG). Bacteria were grown for 20 h at 18 °C, and cells were harvested by centrifugation at 7,000×g for 25 min at 4 °C. Cell pellets were resuspended in lysis buffer (20 mM Tris-Cl (pH 8.0), 500 mM NaCl). Cells were lysed by sonication and the lysate was clarified by centrifugation at 30,000×g for 45 min at 4 °C. The supernatant was loaded on to a 5 mL His-Trap Ni-NTA column. Column was washed extensively with wash buffer (20 mM Tris-Cl (pH 8.0), 500 mM NaCl, 30 mM imidazole) and protein was eluted using a linear gradient to 100% elution buffer (20 mM Tris-Cl (pH 8.0), 500 mM NaCl, 250 mM imidazole). Purity of eluent fractions were checked by SDS-PAGE, and fractions containing protein of interest were pooled and dialyzed into 1 L of dialysis buffer (20 mM Tris-Cl (pH 8.9), 100 mM KCl, 10% glycerol) at 4 °C overnight. Protein concentrations were measured by Bradford assay and aliquots were frozen in liquid nitrogen and stored at -80 °C.

Metabolite extraction and reverse-phase LC/MS data acquisition

Stylissa sp. sponge specimens were collected from Anae Island in Guam in July 2015 at a depth of 10 feet. *Axinella* sp. sponge specimens were collected from the Solomon Islands in April 2018 at a depth of 20 feet. Frozen sponge tissues were lyophilized to dryness and metabolites extracted in 1:1 v/v DCM/MeOH (1 mL solvent/100 mg dry sponge tissue) for 48 h at room temperature. The organic extract was clarified by centrifugation, dried, resuspended in MeOH, and analyzed using an Agilent 1290 Infinity II ultra-performance liquid chromatography (UPLC) coupled to a Bruker ImpactII ultra-high-resolution

Qq-ToF mass spectrometer equipped with an electron spray ionization (ESI) source. A Kinetex 1.7 µm C_{18} reversed phase UPLC column (50×2.1 mm) was used for chromatographic separation. Data were acquired in positive ionization mode, *m/z* 50–2000 Da. An active exclusion of four spectra was employed. Chromatography solvent A: water + 0.1% v/v formic acid, solvent B: MeCN + 0.1% v/v formic acid. Flow rate was held constant at 0.5 mL/min. The elution profile employed was as follows: 2% solvent B for 3 min, a linear gradient from 2% to 50% B in 5 min, 50% B for 2 min, from 50% to 100% B in 5 min, 100% B for 3 min, from 100% to 5% B in 1 min, 5% B for 1 min, from 5% to 100% B in 1 min, 100% B for 3 min, from 100% to 5% B in 1 min, 5% B for 5 min. LC/MS data were converted to lock mass corrected mzXML format using Bruker DataAnalysis software.

Peptide macrocyclization assays with PCY1

Peptide macrocyclization assays were set up using previously described conditions[1]: 300 µM substrate peptide, 2 µM PCY1, 20 mM CAPSO (pH 9.5), 100 mM NaCl, 2 mM DMSO and 5 mM DTT at 30 °C. After 2 h, assays were quenched by addition of equal volume of 5% v/v trichloroacetic acid (TCA) in MeCN and centrifugated to remove precipitates. Samples were analyzed using 1290 Infinity II UPLC system (Agilent Technologies) coupled to a high-resolution Impact II Qq-TOF mass spectrometer (Bruker Daltonics). Mass spectrometry data were collected in the positive ionization mode in the mass range *m/z* 100–2000 Da. A Kinetex™ 1.7 µm C18 reversed phase UHPLC column (50 × 2.1 mm) at a flow rate of 0.5 mL/min was employed and the chromatographic separation was achieved using solvent A: H_2O + 0.1% (v/v) formic acid, and solvent B: MeCN + 0.1% (v/v) formic acid. The chromatography profile was as follows: 5% solvent B from 0–5 min, linear gradient to 100% solvent B from 5–27 min, 100% solvent B from 27–29 min, linear gradient to 5% solvent B from 29–30 min, 5% solvent B from 30–31 min, linear gradient to 100% solvent B from 31–32 min, 100% solvent B from 32–33 min, linear gradient to 5% solvent B from 33–34 min, and 5% solvent B from 34–35 min.

LC-MS method development for one Leu/Ile containing PRMPs

LC/MS data were acquired using a Waters Corporation CORTECS UPLC T3 column (2.1×150 mm, 1.6 µm particle size) coupled to a high-resolution accurate mass Orbitrap ID-X tribrid mass spectrometer. The chromatographic method for sample analysis involved elution with water with 10 mM ammonium formate and 0.1% formic acid (mobile phase A) and MeCN and 0.1% formic acid (mobile phase B) using the following gradient program: 0 min 10% B; 0.5 min 10% B; 8 min 97% B; 10.9 min

97% B; 11 min 10% B; 12 min 10% B. The flow rate was set at 0.4 mL/min. The column temperature was set to 40 °C, and the injection volume was 2.0 µL.

The Orbitrap ID-X is a tribrid spectrometer that utilizes quadrupole isolation with dual detectors, an orbitrap and an ion trap, with a maximum resolving power of 500,000 full width at half maximum (FWHM) at m/z 200 and mass accuracy of <1 ppm. The heated electrospray ionization (HESI) source was operated at a vaporizer temperature of 275 °C, a spray voltage of 3.5 kV, and sheath, auxiliary, and sweep gas flows of 40, 8, and 1 in arbitrary units, respectively. The instrument acquired full MS data in the 100–1000 m/z range in positive ionization mode with an orbitrap resolution of 120,000. Targeted MS[3] data was acquired in the ion trap, with the MS[1] precursor ions isolated in the quadrupole with an isolation window of 1.6 m/z and activated at Higher-energy collisional dissociation (HCD) energy of 55%; and the MS[2] precursor ions isolated in the ion trap with an isolation window of 2 m/z and activated at HCD collision energy of 8%. This method was conserved across all single Leu/Ile containing cyclopeptides reported in this study.

For retention time matching and spiking experiments, we used the Thermo Scientific Accucore Phenyl-X column (2.1 x 50 mm, 2.6 µM particle size) to achieve better chromatographic separation. The chromatographic method involved elution with water with 10 mM ammonium formate and 0.1% formic acid (mobile phase A) and MeCN and 0.1% formic acid (mobile phase B) using the following gradient program: 0 min 10% B; 0.5 min 25% B; 4.7 min 60% B; 5 min 97% B; 7 min 97% B; 7.1 min 10% B; 8 min 10% B. The flow rate was set at 0.5 mL/min. The column temperature was set to 40 °C, and the injection volume was 5.0 µL.

LC-MS method development for two Leu/Ile containing PRMPs

LC/MS data were acquired using a Thermo Scientific Accucore C8 column (2.1×150 mm, 2.6 µm particle size) coupled to a high-resolution accurate mass Orbitrap ID-X tribrid mass spectrometer. The chromatographic method for sample analysis involved elution with water with 10 mM ammonium acetate and 0.1% acetic acid (mobile phase A) and 90:10 isopropanol:water with 10 mm ammonium acetate (mobile phase B) using the following gradient program: 0 min 5% B; 0.2 min 10% B; 1 min 20% B; 7.2 min 40% B; 9 min 97% B; 10.9 min 97% B; 11 min 5% B; 12 min 5% B. The flow rate was set at 0.5 mL/min. The column temperature was set to 40 °C, and the injection volume was 5.0 µL.

The orbitrap was operated with the same ESI source parameters as described in previous section. The instrument acquired full MS data in the 100–1000 m/z range in positive ionization mode with an orbitrap resolution of 120,000. Targeted MS[2] data were collected for the MS[1] precursor ions

corresponding to the cyclopeptide with both activation by HCD collision energy at 30% and CID collision energy at 35%. This was done to ensure detection of most of the MS^2 fragments required for downstream fragmentation analysis. Based on the selection of fragment ions detected in the MS^2 spectra, the hybrid tMS^3 and dd-MS^4 method was developed for each of the selected MS^2 precursor ions. For the *m/z* 679 Da MS^2 precursor ion for PRMP cyclo(FYS**X^1**A**X^2**P), targeted MS^3 data were acquired in the ion trap, with the MS^1 precursor ions isolated in the quadrupole with an isolation window of 1.6 *m/z* and activated at CID collision energy of 35% (CID activation time of 10 ms); and the MS^2 precursor ions were isolated in the ion trap with an isolation window of 2 *m/z* and activated at HCD collision energy of 55%. MS^4 data were acquired in a data-dependent acquisition method, with the MS^3 precursor ions activated with HCD collision energy of 15% and isolated with an isolation window of 2 *m/z*. For the *m/z* 185 Da MS^2 precursor ion for cyclo(FYS**X^1**A**X^2**P), targeted MS^3 data were acquired in the ion trap, with the MS^1 precursor ions isolated in the quadrupole with an isolation window of 1.6 *m/z* and activated at HCD collision energy of 35%; and the MS^2 precursor ions isolated in the ion trap with an isolation window of 2 *m/z* and activated at HCD collision energy of 55%. dd-MS^4 data were acquired with the MS^3 precursor ions activated with HCD collision energy of 15 % and isolated with an isolation window of 3 *m/z*.

For PRMP cyclo(FFPELLP), two fragments *m/z* 340 Da and *m/z* 211 Da were selected for tMS^3 and dd-MS^4 analysis. For both the ions, tMS^3 data were acquired in the ion trap, with the MS^1 precursor ions isolated in the quadrupole with an isolation window of 5 *m/z* and activated at HCD collision energy of 40%; and the MS^2 precursor ions isolated in the ion trap with an isolation window of 5 *m/z* and activated at HCD collision energy of 55%. dd-MS^4 data were acquired with the MS^3 precursor ions activated with HCD collision energy of 15% and isolated with an isolation window of 5 *m/z*.

For PRMP cyclo(WVPLTPLP), two fragments *m/z* 694 Da and *m/z* 308 Da were selected for tMS^3 and dd-MS^4 analysis. For the *m/z* 694 Da fragment, tMS^3 data were acquired in the ion trap, with the MS^1 precursor ions isolated in the quadrupole with an isolation window of 5 *m/z* and activated at CID collision energy of 35%; and the MS^2 precursor ions isolated in the ion trap with an isolation window of 5 *m/z* and activated at HCD collision energy of 55%. dd-MS^4 data were acquired with the MS^3 precursor ions activated with HCD collision energy of 15% and isolated with an isolation window of 5 *m/z*. For the *m/z* 308 Da fragment, tMS^3 data were acquired in the ion trap, with the MS^1 precursor ions isolated in the quadrupole with an isolation window of 5 *m/z* and activated at HCD collision energy of 30%; and the MS^2 precursor ions isolated in the ion trap with an isolation window of 5 *m/z* and activated at HCD collision energy of 55%. dd-MS^4 data were acquired with the MS^3 precursor ions activated with HCD collision energy of 15% and isolated with an isolation window of 5 *m/z*.

For PRMP cyclo(YPIFPIP), two fragments *m/z* 455 Da and *m/z* 308 Da were selected for tMS^3 and dd-MS^4 analysis. For both *m/z* 455 Da and *m/z* 308 Da, tMS^3 data were acquired in the ion trap, with the MS^1 precursor ions isolated in the quadrupole with an isolation window of 5 *m/z* and activated at HCD collision energy of 30%; and the MS^2 precursor ions isolated in the ion trap with an isolation window of 5 *m/z* and activated at HCD collision energy of 55%. dd-MS^4 data were acquired with the MS^3 precursor ions activated with HCD collision energy of 15% and isolated with an isolation window of 5 *m/z*.

Samples for the spiking experiment were prepared by adding crude sponge extract to the synthetic standards in 1:10 (v/v) ratio and the data were acquired using a Thermo Scientific Accucore C8 column (2.1×150 mm, 2.6 µm particle size) with the same LC gradient as described previously. **LC-MS method development for three Leu/Ile containing PRMPs**

LC/MS data were acquired using a Thermo Scientific Accucore Phenyl-X column (2.1 x 50 mm, 2.6 µM particle size) coupled to a high-resolution accurate mass Orbitrap ID-X tribrid mass spectrometer. The chromatographic method for sample analysis involved elution with water with 10 mM ammonium formate and 0.1% formic acid (mobile phase A) and MeCN and 0.1% formic acid (mobile phase B) using the following gradient program: 0 min 20% B; 7 min 100% B; 10.5 min 100% B; 10.7 min 20% B; 12 min 20% B. The flow rate was set at 0.4 mL/min. The column temperature was set to 40 °C, and the injection volume was 2.0 µL.

The orbitrap was operated with the same ESI source parameters as described in previous sections. The instrument acquired full MS data in the 100–1000 *m/z* range in positive ionization mode with an orbitrap resolution of 120,000. tMS^2, tMS^3 and dd-MS^4 data were acquired for the MS^1 precursor ion corresponding to the cyclopeptide similar to the method as described above for two Leu/Ile containing cyclopeptides. For the *m/z* 875 Da and *m/z* 608 Da MS^2 precursor ions for cyclo(**X^1**PHPY**X^{2}X^3**GP), targeted MS^3 data were acquired in the ion trap, with the MS^1 precursor ions isolated in the quadrupole with an isolation window of 1.6 *m/z* and activated at CID collision energy of 35% (CID activation time of 10 ms); and the MS^2 precursor ions isolated in the ion trap with an isolation window of 2 *m/z* and activated at HCD collision energy of 55%. MS^4 data were acquired in a data-dependent acquisition mode, with the MS^3 precursor ions activated with HCD collision energy of 15% and isolated with an isolation window of 2 *m/z*. For the *m/z* 211 Da MS^2 precursor ion, tMS^3 data were acquired in the ion trap, with the MS^1 precursor ions isolated in the quadrupole with an isolation window of 1.6 *m/z* and activated at HCD collision energy of 40%; and the MS^2 precursor ions isolated in the ion trap with an isolation window of 2 *m/z* and activated at HCD collision energy of 55%. dd-MS^4 data were acquired with the MS^3 precursor ions activated with HCD collision energy of 15% and isolated with an isolation window of 5 *m/z*.

For the cyclo(WLPLTPLP) PRMP, three MS^2 fragment ions, m/z 308, m/z 312, and m/z 397 Da were selected for tMS^3 and dd-MS^4 analysis. The same method was used for all the precursor ions with tMS^3 data acquired in the ion trap, and the MS^1 precursor ions isolated in the quadrupole with an isolation window of 1.6 m/z and activated at HCD collision energy of 40%; and the MS^2 precursor ions isolated in the ion trap with an isolation window of 2 m/z and activated at HCD collision energy of 55%. dd-MS^4 data were acquired with the MS^3 precursor ions activated with HCD collision energy of 15% and isolated with an isolation window of 5 m/z.

For the retention time matching experiment, data was acquired on a Thermo Scientific Accucore C30 column (2.1×150 mm, 2.6 µm particle size) for better resolving power between the standards. The chromatographic method for sample analysis involved elution with water with 10 mM ammonium acetate and 0.1% acetic acid (mobile phase A) and 90:10 isopropanol:water with 10 mm ammonium acetate (mobile phase B) using the following gradient program: 0 min 15% B; 1 min 15% B; 7 min 32% B; 7.8 min 100% B; 10.5 min 100% B; 10.7 min 15% B; 12 min 15% B. The flow rate was set at 0.4 mL/min. The column temperature was set to 40 °C, and the injection volume was 2.0 µL.

Microbiome sequencing and analyses

The procedure for querying the sponge-associated microbiome was based on our previous reports.[2] The raw sequence reads were demultiplexed and sequence variants (SVs) generated by QIIME2 using the qiime tools import script, qiime demux script and the DADA2 plugin,[3] respectively. Based on quality scores, the forward and reverse reads were truncated at 180 bp using the qiime dada2 denoise script. Taxonomy was assigned using the SILVA pre-trained classifier using the qiime feature classifier plug-in.[4] The qiime taxa barplot script was used to generate the bar plots representing the taxonomic distribution. The α-diversity of the microbiome was quantified by computing Shannon index using the q2_diversity plugin in QIIME2.
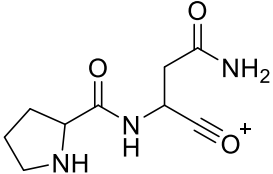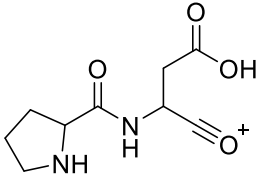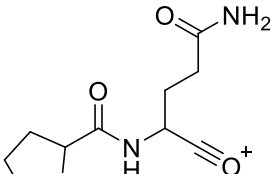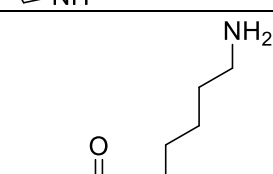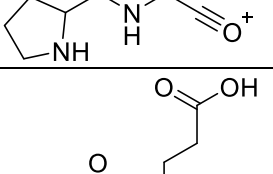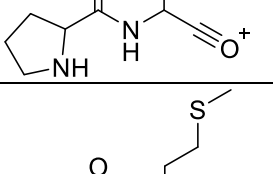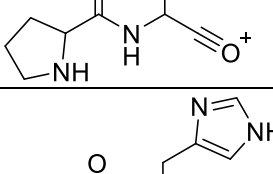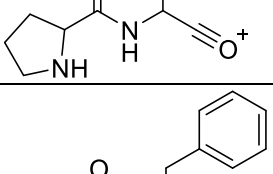
Data availability

Mass spectrometry data has been deposited to the MassIVE repository (**https://massive.ucsd.edu/**) under the accession code MSV000087277.

Table S1: $[M+H]^{1+}$ masses and structures of the ^{N}Pro-Xaa^C dipeptide MS^2 ions

^{N}**Pro-Xaa^C** $[M+H]^{1+}$	Structure
^{N}Pro-Gly^C 155.0815	
^{N}Pro-Ala^C 169.0972	
^{N}Pro-Ser^C 185.0921	
^{N}Pro-Pro^C 195.1128	
^{N}Pro-Val^C 197.1285	
^{N}Pro-Thr^C 199.1077	
^{N}Pro-Cys^C 201.0692	
^{N}Pro-Ile^C 211.1441	
^{N}Pro-Leu^C 211.1441	

^NPro-Asn^C 212.1030	
^NPro-Asp^C 213.0870	
^NPro-Gln^C 226.1186	
^NPro-Lys^C 226.1550	
^NPro-Glu^C 227.1026	
^NPro-Met^C 229.1005	
^NPro-His^C 235.1190	
^NPro-Phe^C 245.1285	
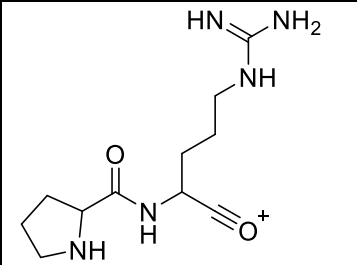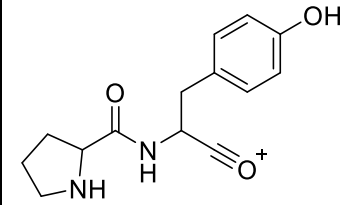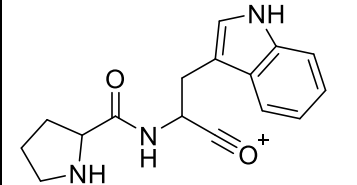
^{N}Pro-Arg^C 254.1612	
^{N}Pro-Tyr^C 261.1234	
^{N}Pro-Trp^C 284.1394	

Table S2: [M+H]$^{1+}$ masses and structures of the amino acyl immonium MS^2 ions

[M+H]$^{1+}$	Structure
30.0338	H$_2$N$^+$=
44.0495	H$_2$N$^+$=
60.0444	H$_2$N$^+$= with OH
70.0651	N$^+$ ring with H
72.0808	H$_2$N$^+$=
74.0600	H$_2$N$^+$= with OH
76.0215	H$_2$N$^+$= with SH
86.0964	H$_2$N$^+$=
86.0964	H$_2$N$^+$=
87.0553	H$_2$N$^+$= with C(=O)NH$_2$
88.0393	H$_2$N$^+$= with C(=O)OH
101.0709	H$_2$N$^+$= with H$_2$N—C=O
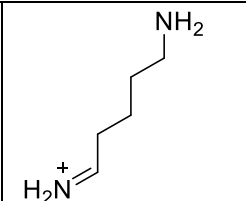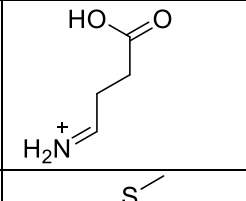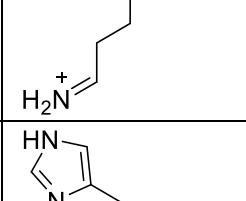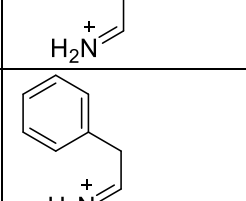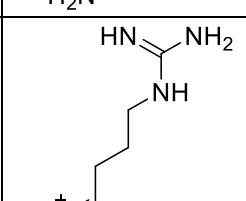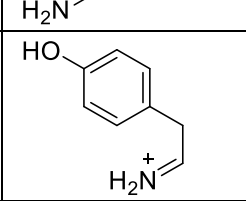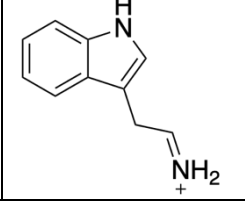
101.1073	
102.0550	
104.0528	
110.0713	
120.0808	
129.1135	
136.0757	
159.0917	

Table S3: Compound names, sequences, sources, and literature references for sponge derived PRMPs. PRMPs sequenced in this study are highlighted in yellow.

PRMP	Sequence	Sponge	Reference DOI
Phakellistatin 1	YPIPIFP	*Phakellia costata*	10.1021/np50092a011
Phakellistatin 2	FPIIPYP	*Phakellia carteri*	10.1016/S0960-894X(01)80781-2
Phakellistatin 3	FGPTLWP	*Phakellia carteri*	10.1021/jo00086a001
Phakellistatin 4	FIFSPTP	*Phakellia costata*	10.3987/COM-94-S45
Phakellistatin 5	FNAMAIP	*Phakellia costata*	10.1016/S0960-894X(01)80108-6
Phakellistatin 6	FPWLPIP	*Phakellia costata*	10.1016/S0960-894X(01)80695-8
Phakellistatin 7	FALPPYIPPI	*Phakellia costata*	10.1016/0960-894X(95)00219-J
Phakellistatin 8	FVLPPYIPPI	*Phakellia costata*	10.1016/0960-894X(95)00219-J
Phakellistatin 9	FVLPPYVPPI	*Phakellia costata*	10.1016/0960-894X(95)00219-J
Phakellistatin 10	WVPLTPIP	*Phakellia* sp.	10.1021/np50120a025
Phakellistatin 11	FPFIFPQP	*Phakellia* sp.	10.1021/np50120a025
Phakellistatin 12	FTLPPYIPPI	*Phakellia* sp.	10.1016/S0960-894X(02)01054-5
Phakellistatin 13	FGPTLWP	*Phakellia fusca*	10.1021/np020223y
Phakellistatin 14	FDAMAIP	*Phakellia* sp.	10.1021/np040092w
Phakellistatin 15	WIPLTPLP	*Phakellia fusca*	10.1021/np9008267
Phakellistatin 16	FDSRAVTYP	*Phakellia fusca*	10.1021/np9008267
Phakellistatin 17	WVPLIPIP	*Phakellia fusca*	10.1021/np9008267
Phakellistatin 18	YPIFPIP	*Phakellia fusca*	10.1021/np9008267
Phakellistatin 20[1]	FNAMAIP	*Stylissa flabelliformis*	10.1021/acs.jnatprod.8b00121
Phakellistatin 21[2]	FELPPYIPPM	*Stylissa flabelliformis*	10.1021/acs.jnatprod.8b00121
Phakellistatin 22	FELPPYIPPM	*Stylissa flabelliformis*	10.1021/acs.jnatprod.8b00121
Fuscasin A	FVLPPPP	*Phakellia fusca*	10.1021/acs.jnatprod.8b01033
Fuscasin B	YALPVNR	*Phakellia fusca*	10.1021/acs.jnatprod.8b01033
Fuscasin C	YPYAPAL	*Phakellia fusca*	10.1021/acs.jnatprod.8b01033
Fuscasin D	YLLPLPD	*Phakellia fusca*	10.1021/acs.jnatprod.8b01033
Hymenamide A	FWRPPVP	*Hymeniacidon* sp.	10.1016/S0040-4020(01)86318-3
Hymenamide B	PNFVEFP	*Hymeniacidon* sp.	10.1016/S0040-4020(01)86318-3
Hymenamide C	FGPELWP	*Hymeniacidon* sp.	10.1016/S0040-4020(01)80422-1
Hymenamide D	YDPLAIP	*Hymeniacidon* sp.	10.1016/S0040-4020(01)80422-1
Hymenamide E	YFFPTTP	*Hymeniacidon* sp.	10.1016/S0040-4020(01)80422-1
Hymenamide F	PAVMLRP	*Hymeniacidon* sp.	10.1016/0040-4020(96)00281-5
Hymenamide G	YVPLILPP	*Hymeniacidon* sp.	10.1016/S0040-4020(01)85006-7
Hymenamide H	WVPLTPLP	*Hymeniacidon* sp.	10.1016/S0040-4020(01)85006-7
Hymenamide J	YDFWKVYP	*Hymeniacidon* sp.	10.1016/S0040-4020(01)85006-7
Hymenamide K	YDFWKAVP	*Hymeniacidon* sp.	10.1016/S0040-4020(01)85006-7
Stylissamide A	YKPPVYP	*Stylissa caribica*	10.1002/ejoc.200700013
Stylissamide B	FPPPIYP	*Stylissa caribica*	10.1002/ejoc.200700013
Stylissamide C	FPFIPYP	*Stylissa caribica*	10.1002/ejoc.200700013
Stylissamide D	FIFYPLP	*Stylissa caribica*	10.1002/ejoc.200700013
Stylissamide E	YPAIQIP	*Stylissa caribica*	10.1021/np900664f
Stylissamide F	FDPRFPP	*Stylissa caribica*	10.1021/np900664f
Stylissamide G	FPLIPFP	*Stylissa caribica*	10.1021/np400891s

[1] The methionine residue in Phakellistatins 20, 21, 22 is oxidized.
[2] Phakellistatins 21 and 22 are epimers at the sulfur atom.

| Stylissamide H	WPISFVP	*Stylissa caribica*	10.1021/np400891s
Stylissamide L	FPPSYPQ	*Stylissa caribica*	10.3390/md18090443
Stylissamide X	WFPLTPIP	*Stylissa* sp.	10.1016/j.bmcl.2011.10.023
Stylisin 1	YPIFPLP	*Stylissa caribica*	10.1021/np060006n
Stylisin 2	FPIPYPP	*Stylissa caribica*	10.1021/np060006n
Stylissatin A	FIYFPIP	*Stylissa massa*	10.1016/j.tetlet.2013.10.003
Stylissatin B	FPPGHPL	*Stylissa massa*	10.1016/j.tetlet.2016.08.024
Stylissatin C	FVLPPPD	*Stylissa massa*	10.1016/j.tetlet.2016.08.024
Stylissatin D	FVLPPPD	*Stylissa massa*	10.1016/j.tetlet.2016.08.024
Stylissatin E	FVPELWP	*Stylissa* sp.	This work
Stylissatin F	FPWVPLTP	*Stylissa* sp.	This work
Stylissatin G	WLPLTPLP	*Stylissa* sp.	This work
Stylostatin 1	FNSLAIP	*Stylissa massa*	10.1021/jo00052a041
Axinellin C	FPLTVPWP	*Stylissa massa*	10.1016/S0040-4020(02)00898-0
Wainunuamide	FPHPPGL	*Stylissa massa*	10.1016/S0040-4039(01)01993-1
Carteritin A	FIPPEYP	*Stylissa carteri*	10.1016/j.tetlet.2016.02.031
Carteritin B	YYPSLYP	*Stylissa carteri*	10.1016/j.tetlet.2016.02.031
Euryjanicin A	WPISFVP	*Prosuberites laughlini*	10.1016/j.tetlet.2009.05.067
Euryjanicin B	FVPPATP	*Prosuberites laughlini*	10.1021/np9004135
Euryjanicin C	FPISIPL	*Prosuberites laughlini*	10.1021/np9004135
Euryjanicin D	FSPIFPI	*Prosuberites laughlini*	10.1021/np9004135
Euryjanicin E	FPIFPIN	*Prosuberites laughlini*	10.1016/j.tet.2013.10.095
Euryjanicin F	FFPIFPI	*Prosuberites laughlini*	10.1016/j.tet.2013.10.095
Euryjanicin G	FPFPIFP	*Prosuberites laughlini*	10.1016/j.tet.2013.10.095
Axinastatin 1	FVVPVNP	*Axinella* sp.	10.1021/jm00115a027
Axinastatin 2	FVLPVNP	*Axinella* sp.	10.1021/jm00034a014
Axinastatin 3	FILPVNP	*Axinella* sp.	10.1021/jm00034a014
Axinastatin 4	LWVPLTP	*Axinella carteri*	10.1021/np970139w
Axinelllin A	FTLFPNP	*Axinella carteri*	10.1002/(SICI)1099-0690(199811)1998:11<2659::AID-EJOC2659>3.0.CO;2-H
Axinellin B	FPTLVPWP	*Axinella carteri*	10.1002/(SICI)1099-0690(199811)1998:11<2659::AID-EJOC2659>3.0.CO;2-H
Axinellin C	FPLTVPWP	*Stylotella aurantium*	10.1016/S0040-4020(02)00898-0
Axinellin D	FFPELWP	*Axinella* sp.	This work
Axinellin E	FYSLAIP	*Axinella* sp.	This work
Axinellin F	FFPELLP	*Axinella* sp.	This work
Axinellin G	IPHPYIIGP	*Axinella* sp.	This work
Reniochalistatin A	LLPNVIP	*Reniochalina stalagmitis*	10.1021/np5006778
Reniochalistatin B	FYLPLPI	*Reniochalina stalagmitis*	10.1021/np5006778
Reniochalistatin C	FPIYFPI	*Reniochalina stalagmitis*	10.1021/np5006778
Reniochalistatin D	FPFIFPP	*Reniochalina stalagmitis*	10.1021/np5006778
Reniochalistatin E	WPVIPIPL	*Reniochalina stalagmitis*	10.1021/np5006778
Stylopeptide 1	FSPIPLI	*Stylotella* sp.	10.1021/jo00130a027
Stylopeptide 2	FPYPTPFLLP	*Stylotella* sp.	10.1021/np0704856
Malaysiatin	FVVVNPP	*Pseudaxinyssa* sp.	10.1016/S0040-4039(00)61115-2
Dominicin	PTPIIILP	*Eurypon laughlini*	10.1021/np049711r
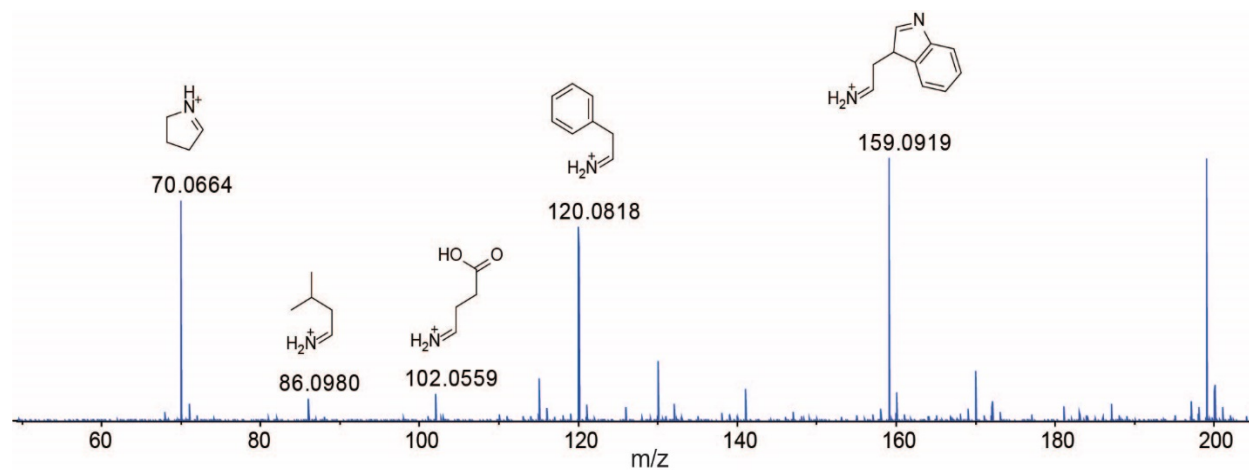
Fig. S1: Annotation of MS^2 amino acyl immonium ions detected for PRMP cyclo(FFPE**X**WP). Residue **X** was determined to be Leu.
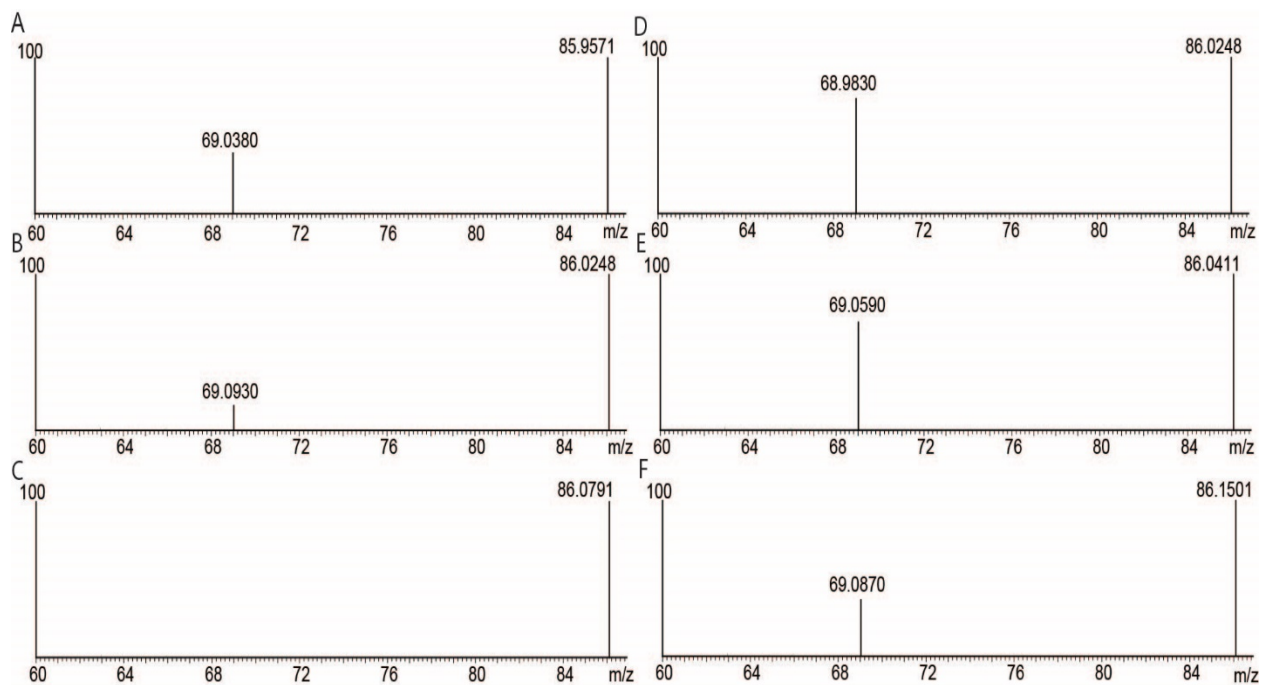
Fig. S2: Abundance of MS³ *m/z* 69 Da product ion detected for synthetic standards with one Leu residue at HCD 15 (**A**), HCD 11 (**B**), HCD 8 (**C**) and one Ile residue at HCD 15 (**D**), HCD 11 (**E**), HCD 8 (**F**). Note that at HCD 8, panels **C** and **F**, the MS³ *m/z* 69 Da product ion is not detected for Leu, but only detected for Ile. For all other HCD energies, some abundance of the MS³ *m/z* 69 Da is detected for the Leu residue.
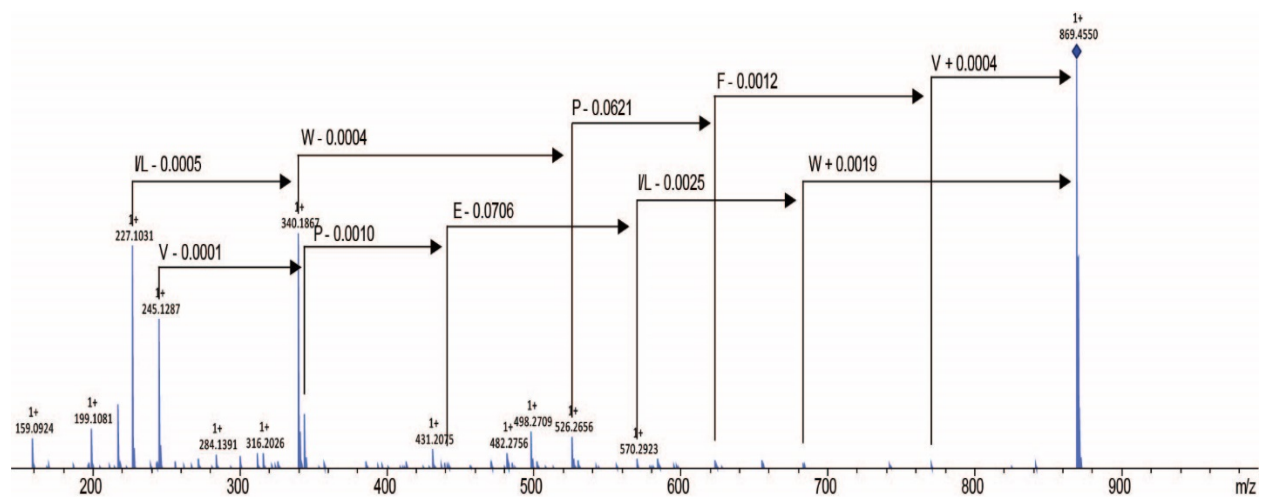
Fig. S3: MS^2 sequencing of PRMP stylissatin E cyclo(FVPE**L**WP).
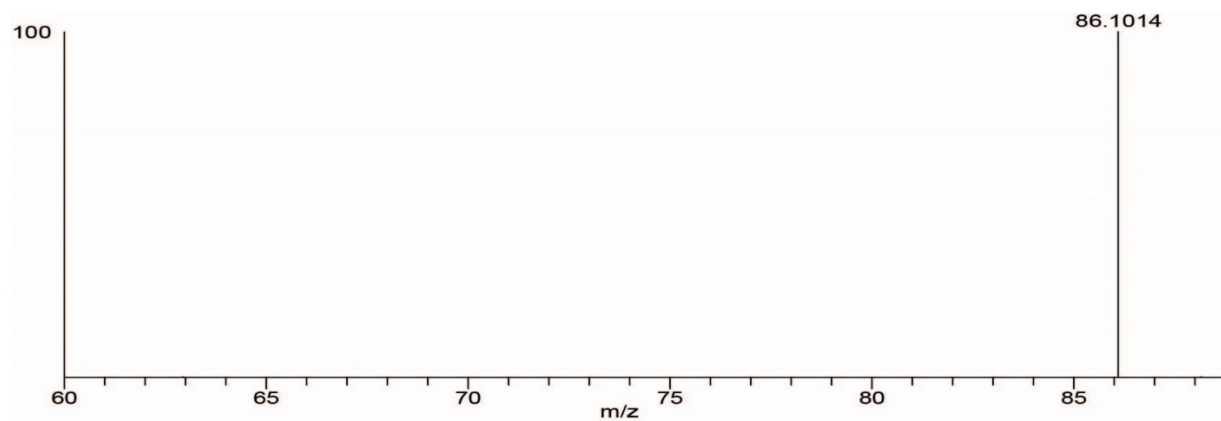
Fig. S4: $MS^2(86) \rightarrow MS^3$ spectra for PRMP stylissatin E cyclo(FVPE**L**WP).
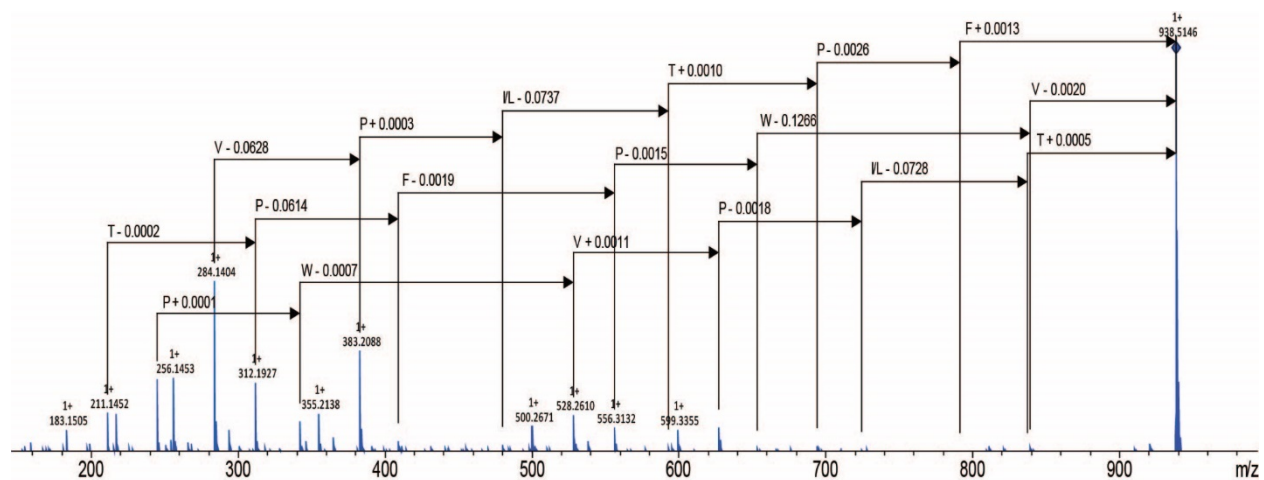
Fig. S5: MS^2 sequencing of PRMP stylissatin F cyclo(FPWVP**L**TP).
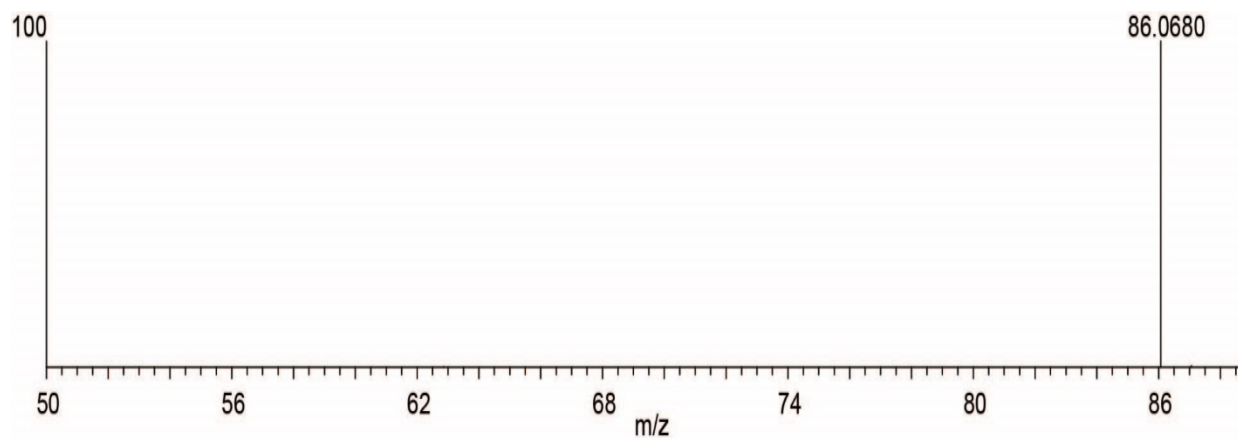
Fig. S6: $MS^2(86) \rightarrow MS^3$ spectra for PRMP stylissatin F cyclo(FPWVP**L**TP).
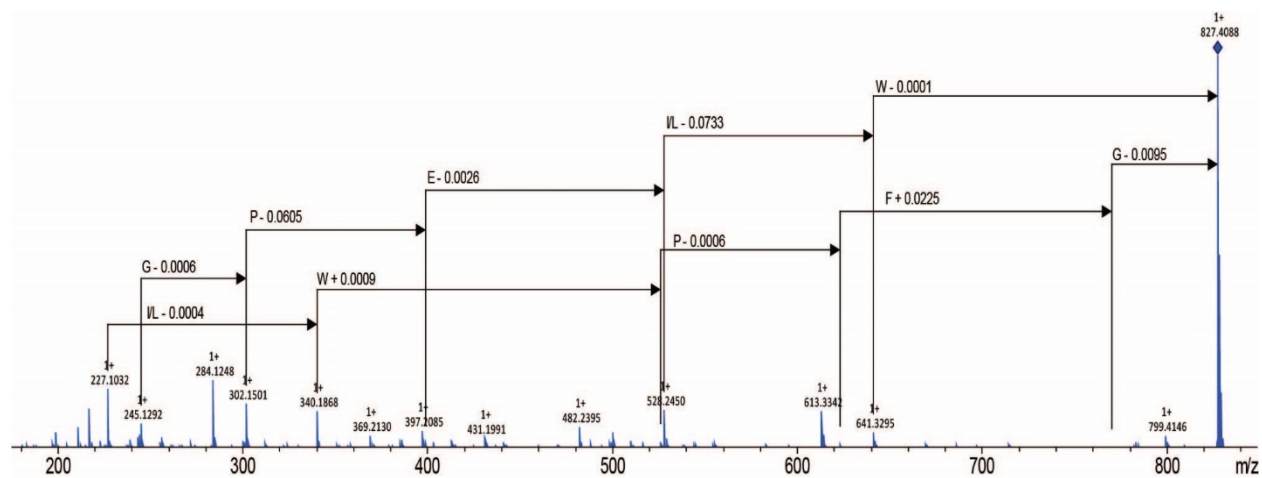
Fig. S7: MS^2 sequencing for PRMP hymenamide C cyclo(FGPE**L**WP).
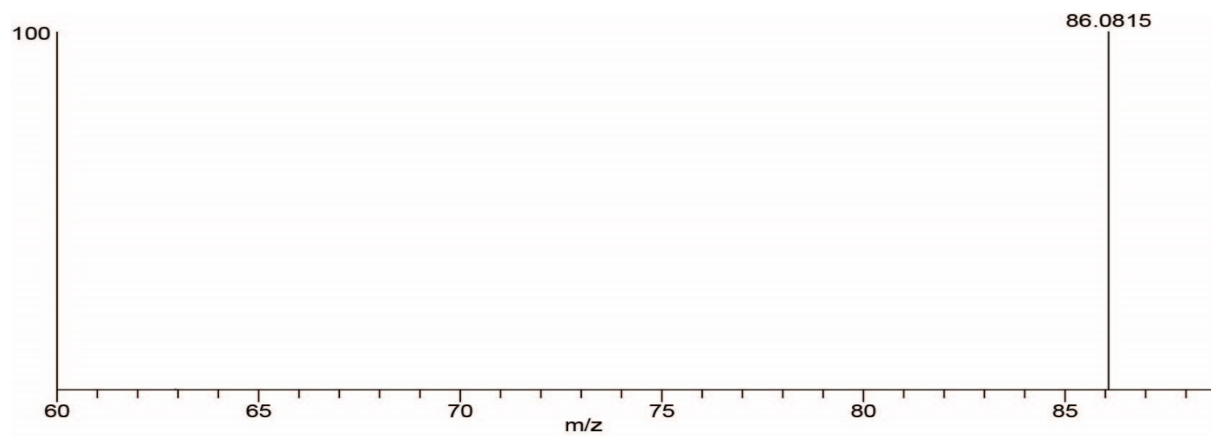
Fig. S8: $MS^2(86) \rightarrow MS^3$ spectra for hymenamide C cyclo(FGPE**L**WP).
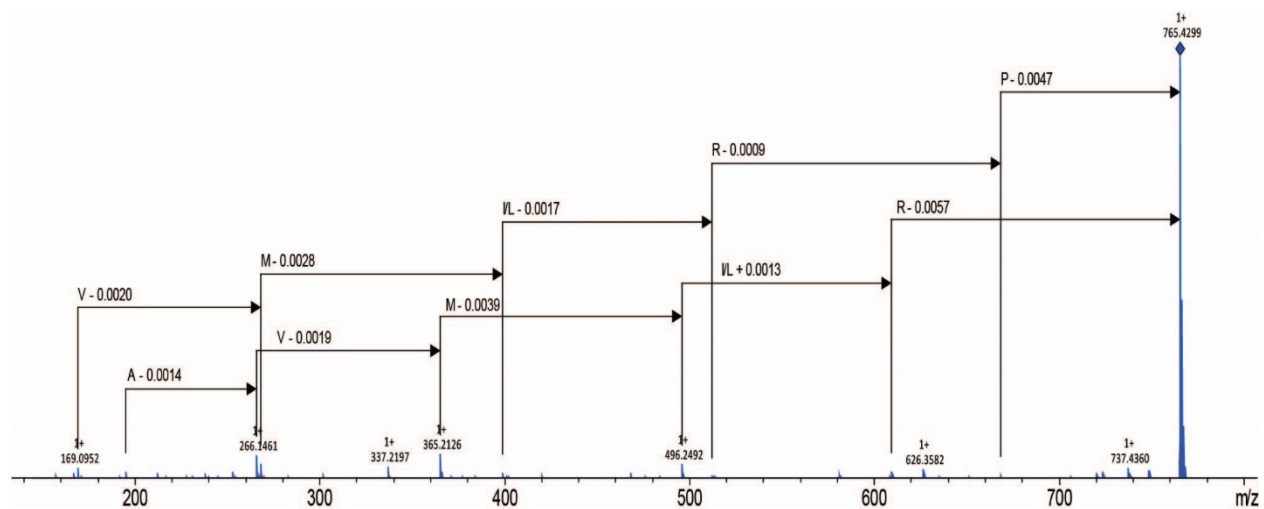
Fig. S9: MS^2 sequencing for PRMP hymenamide F cyclo(PAVMLRP).
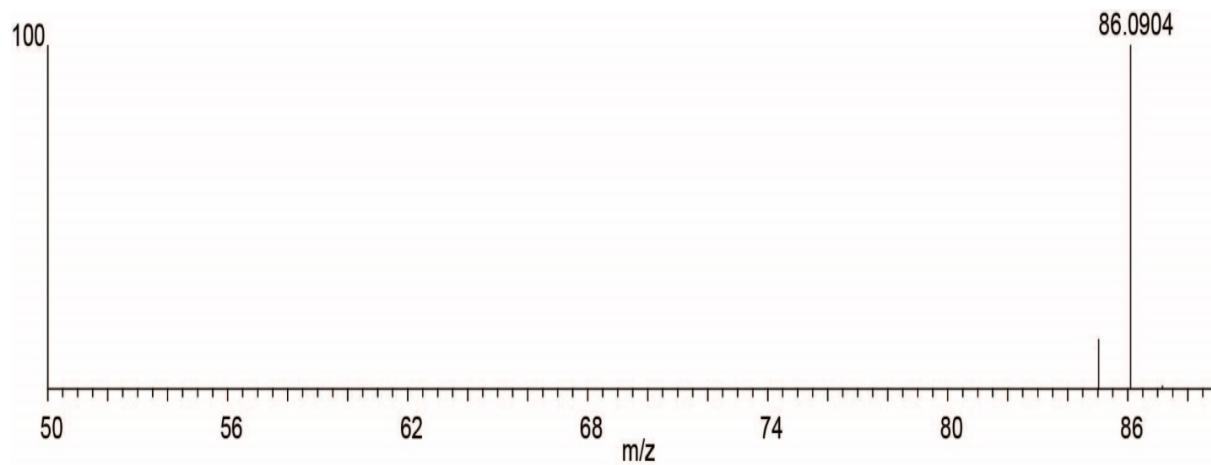
Fig. S10: $MS^2(86) \rightarrow MS^3$ spectra for PRMP hymenamide F cyclo(PAVMLRP).
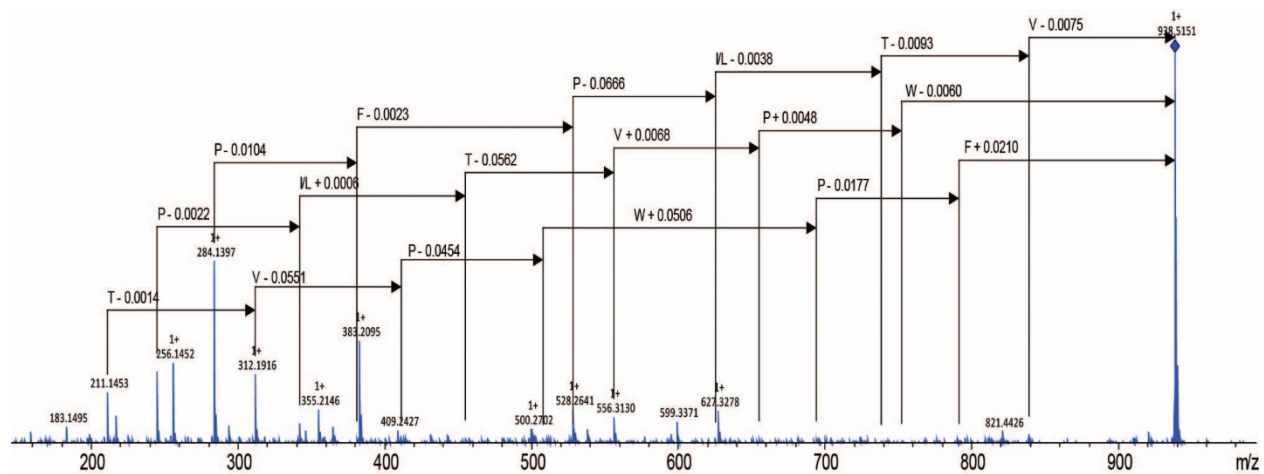
Fig. S11: MS^2 sequencing for PRMP axinellin B cyclo(FP**L**TVPWP).
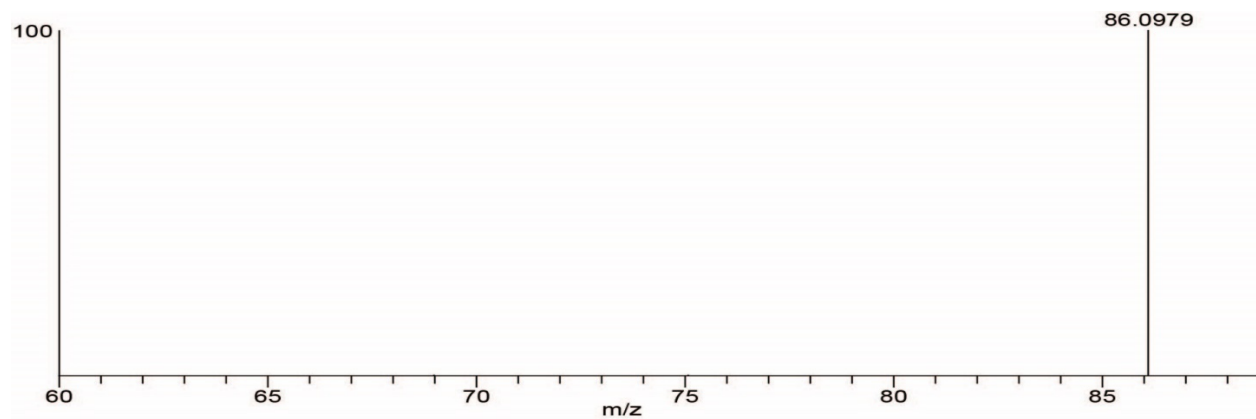
Fig. S12: MS^2(86)→MS^3 spectra for PRMP axinellin B cyclo(FP**L**TVPWP).
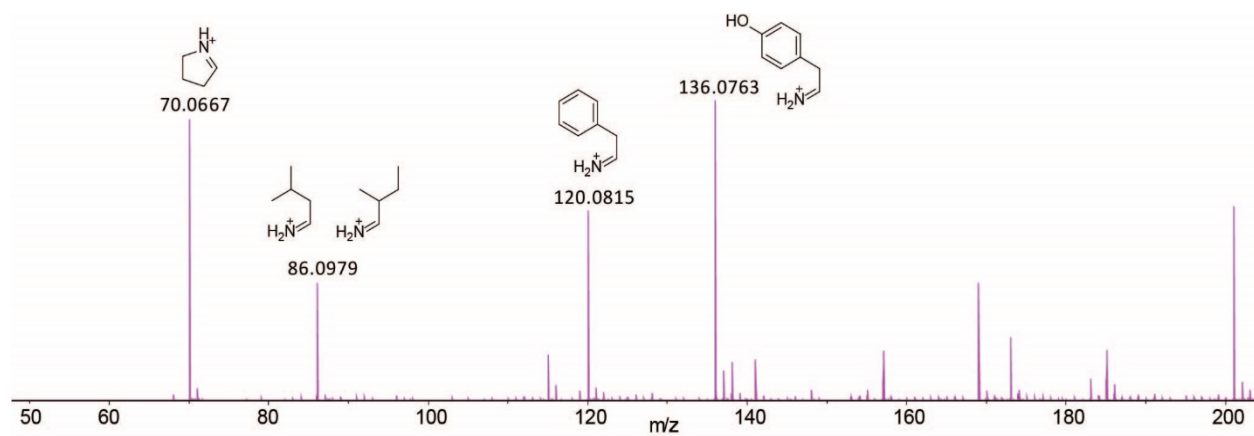
Fig. S13: Annotation of amino acyl immonium ions detected in the MS^2 spectra for PRMP axinellin E cyclo(FYSLAIP). Immonium product ions for Ala and Ser residues were not detected.
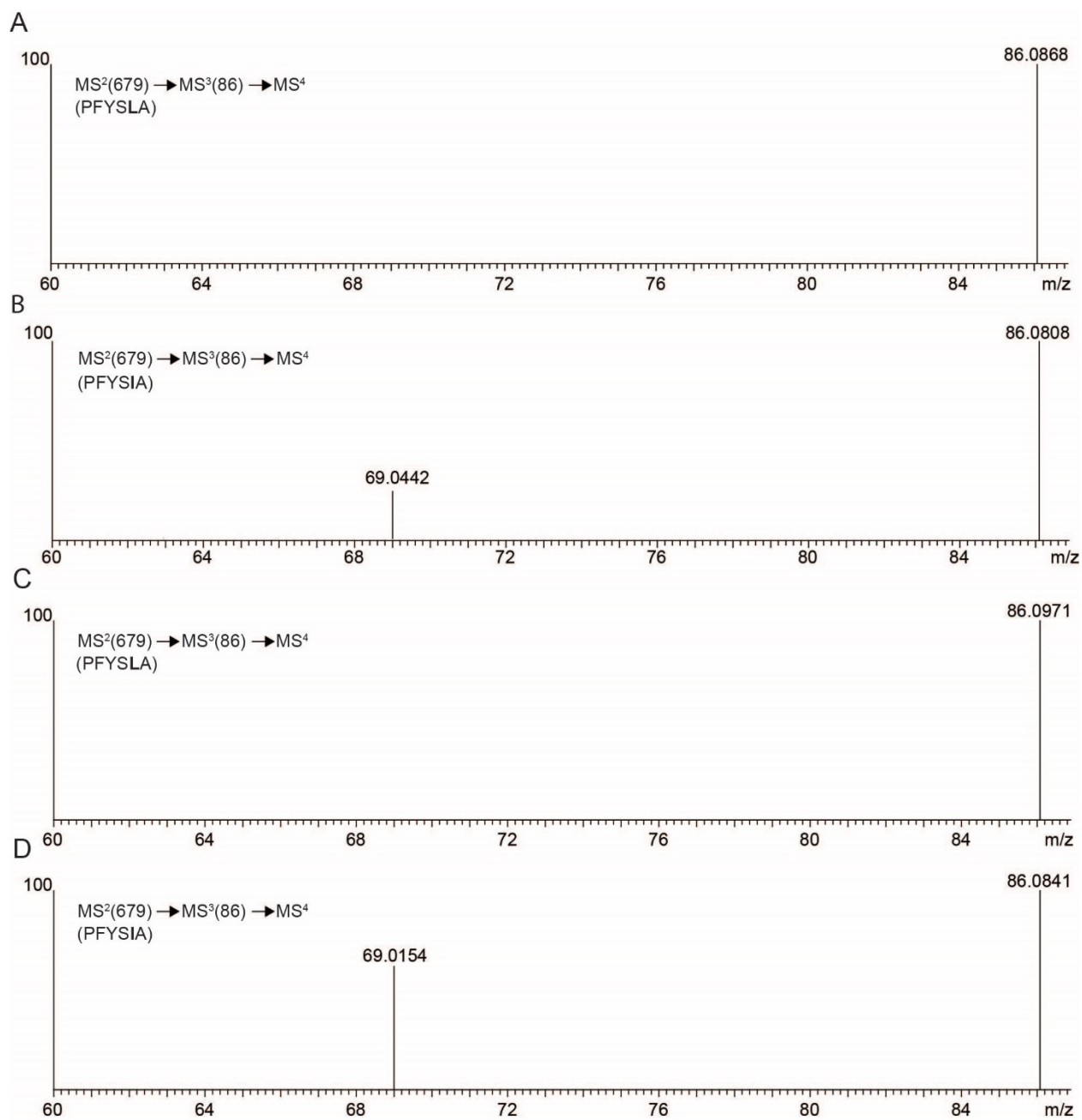
Fig. S14: $MS^2(679) \rightarrow MS^3(86) \rightarrow MS^4$ spectra for standards, (**A**) cyclo(FYSLALP), (**B**) cyclo(FYSIALP), (**C**) cyclo(FYSLAIP), and (**D**) cyclo(FYSIAIP).
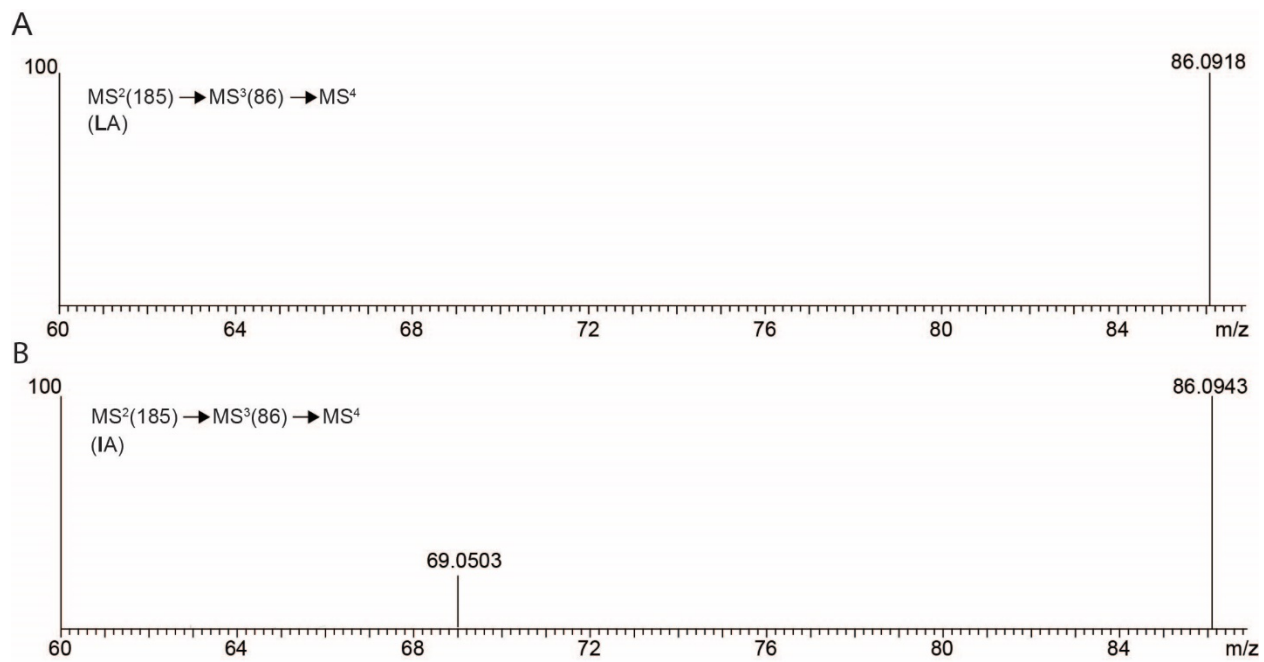
Fig. S15: $MS^2(185) \rightarrow MS^3(86) \rightarrow MS^4$ spectra for standards (**A**) cyclo(FYSLA**L**P), and (**B**) cyclo(FYSLA**I**P). Note that for both these standards, X^1=Leu.
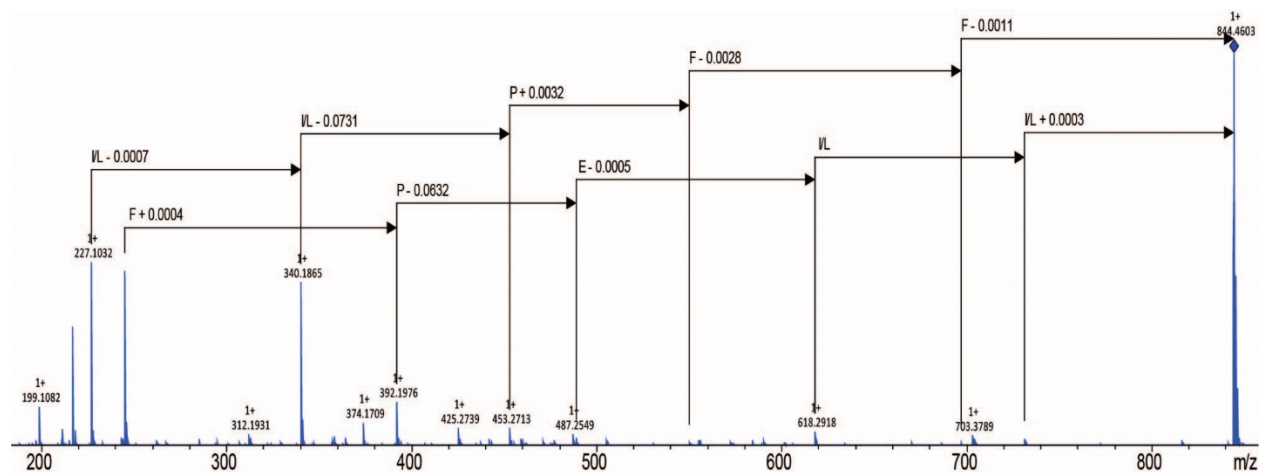
Fig. S16: MS^2 sequencing of PRMP axinellin F cyclo(FFPE**LL**P).
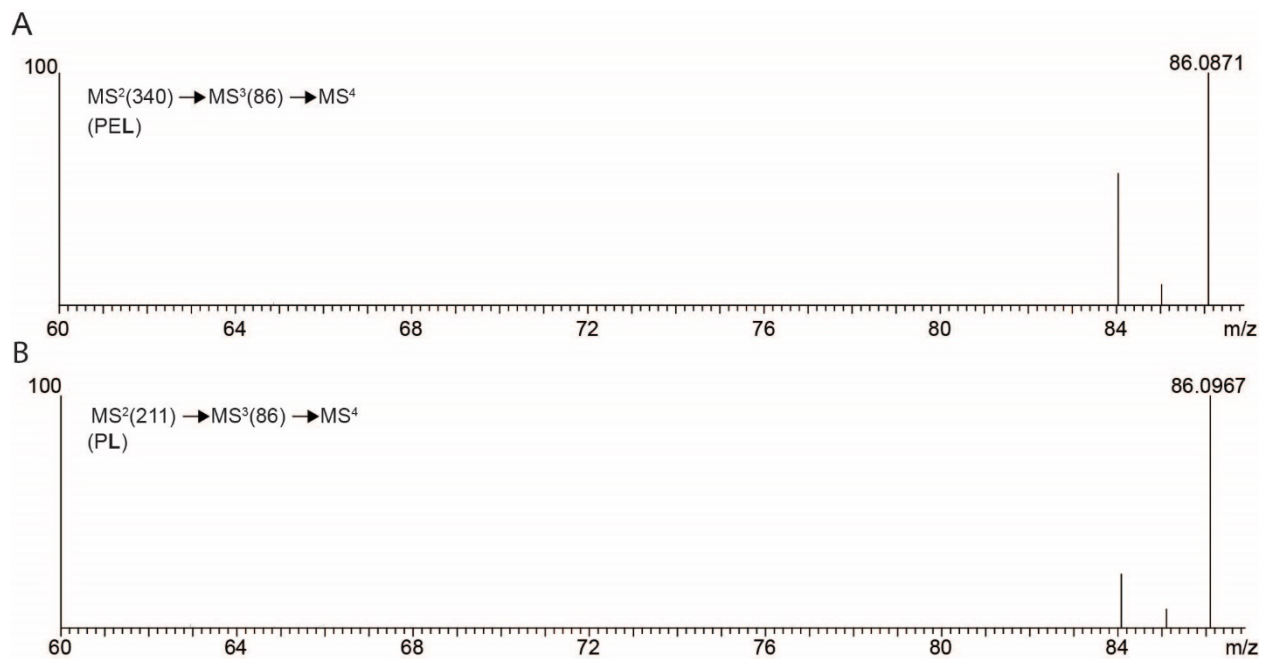
Fig. S17: (**A**) $MS^2(340) \rightarrow MS^3(86) \rightarrow MS^4$ and (**B**) $MS^2(211) \rightarrow MS^3(86) \rightarrow MS^4$ spectra for PRMP cyclo(FFPE**LL**P).
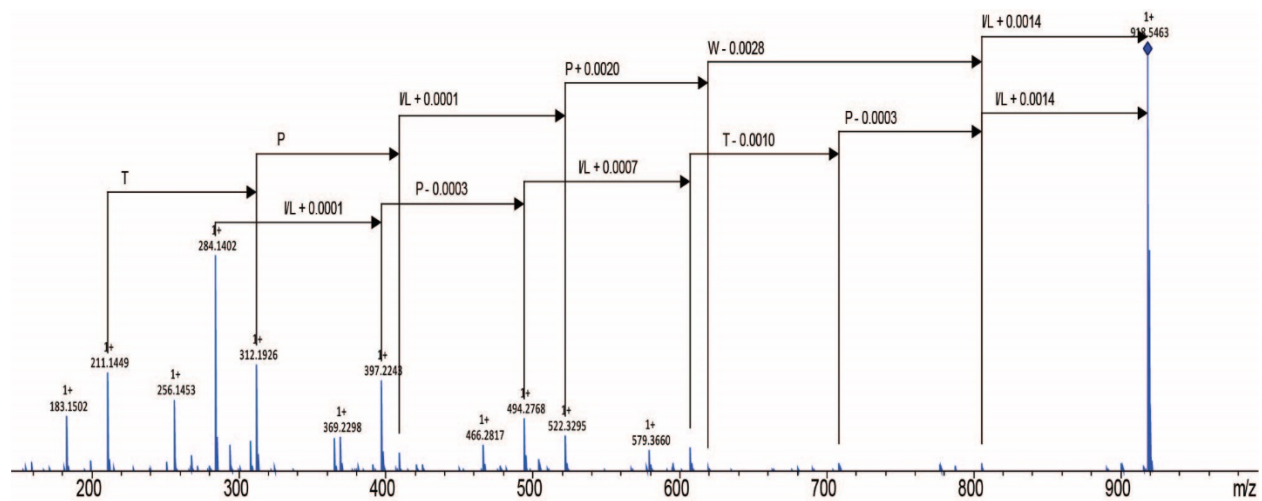
Fig. S18: MS^2 sequencing of PRMP stylissatin G cyclo(WL**P**LTP**L**P).
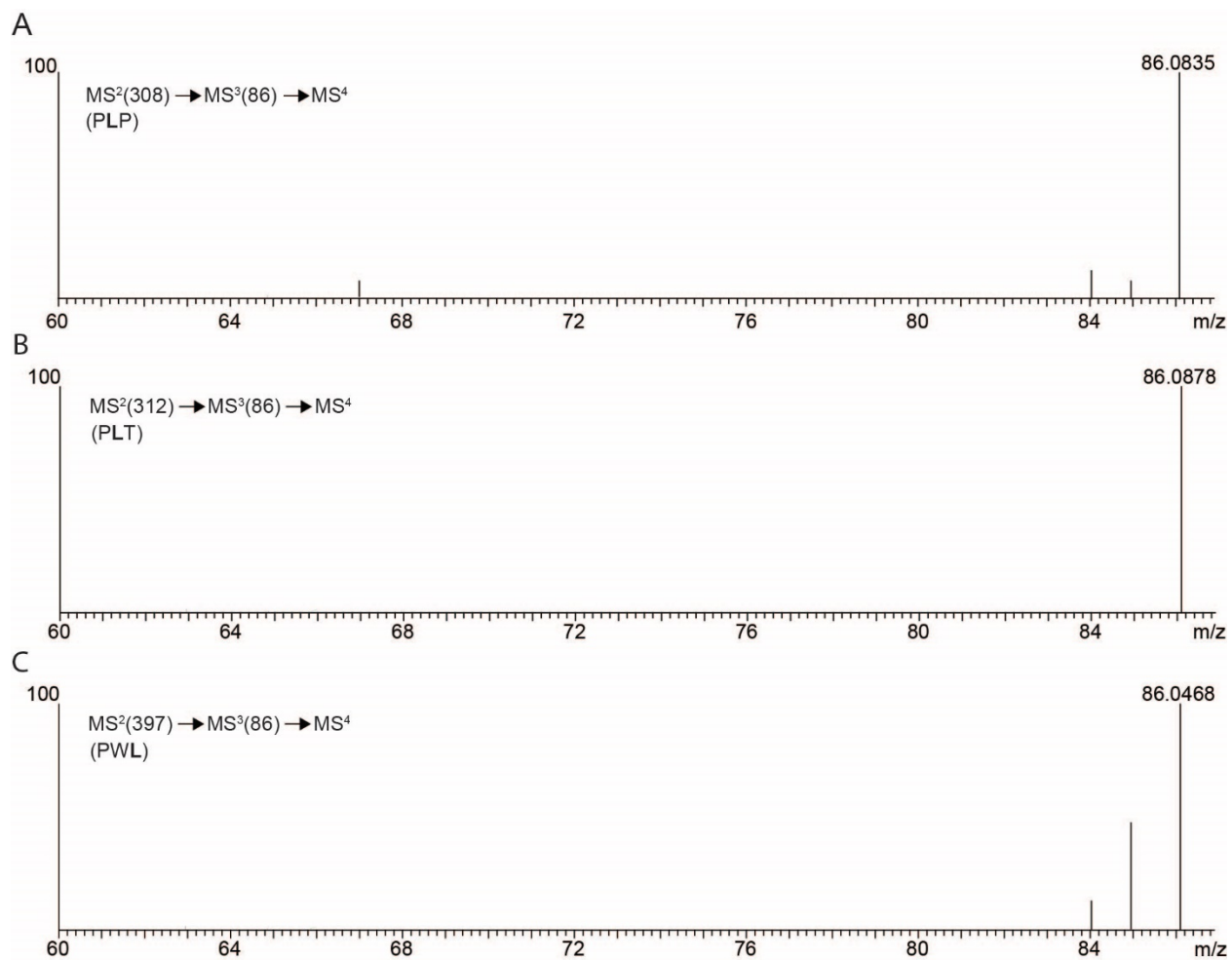
Fig. S19: (**A**) $MS^2(308){\rightarrow}MS^3(86){\rightarrow}MS^4$ (**B**) $MS^2(312){\rightarrow}MS^3(86){\rightarrow}MS^4$ (**C**) $MS^2(397){\rightarrow}MS^3(86){\rightarrow}MS^4$ spectra for PRMP cyclo(W**L**PLTPLP).
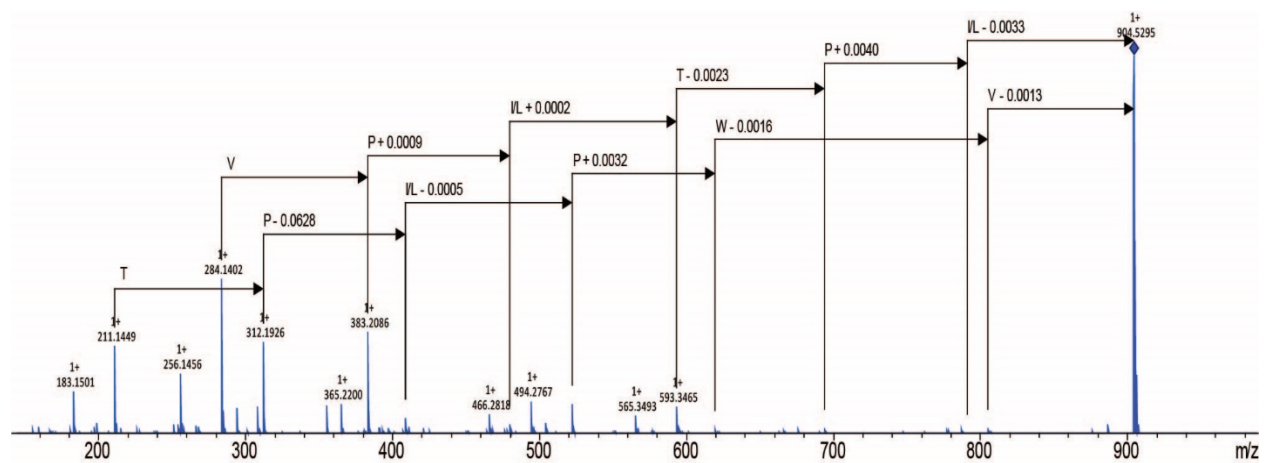
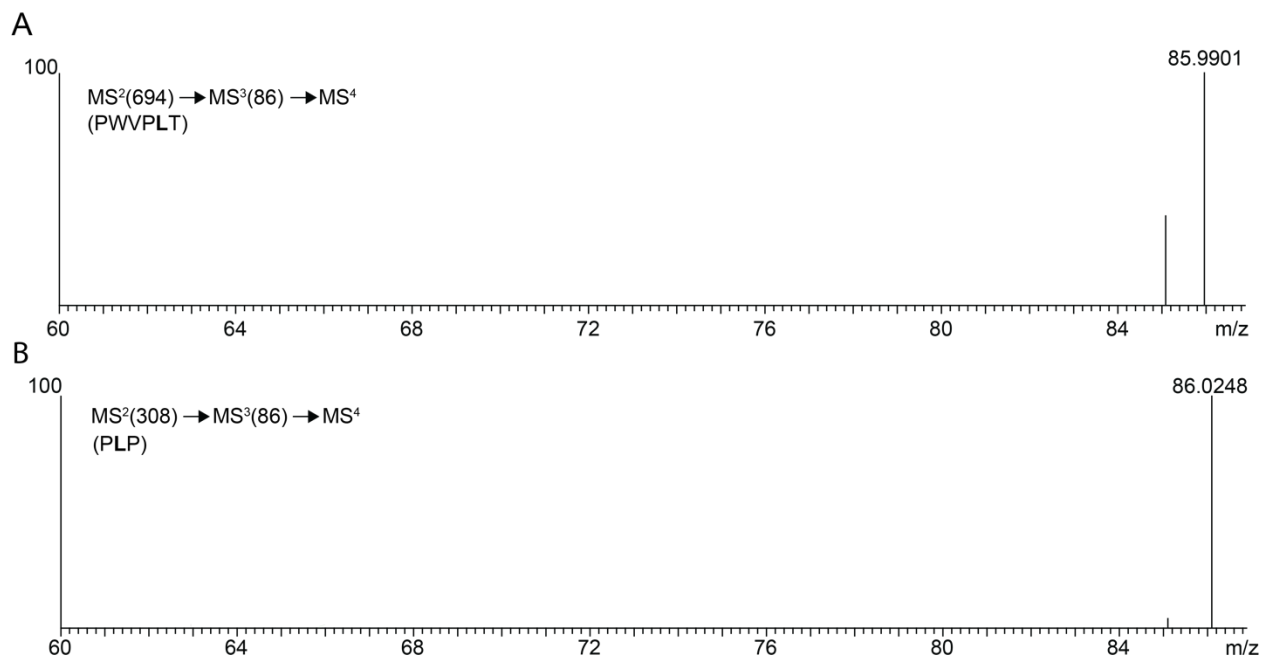**Fig. S20**: MS^2 sequencing of PRMP hymenamide H cyclo(WVP**L**TP**L**P).

Fig. S21: (**A**) $MS^2(694) \rightarrow MS^3(86) \rightarrow MS^4$ (**B**) $MS^2(308) \rightarrow MS^3(86) \rightarrow MS^4$ analysis of PRMP cyclo(WVP**L**TP**L**P).
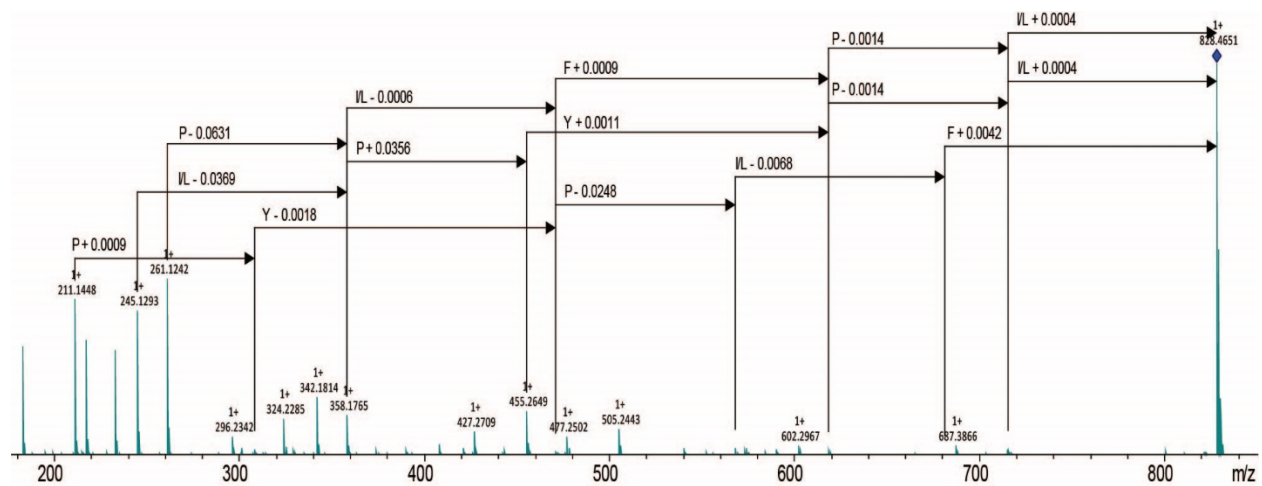
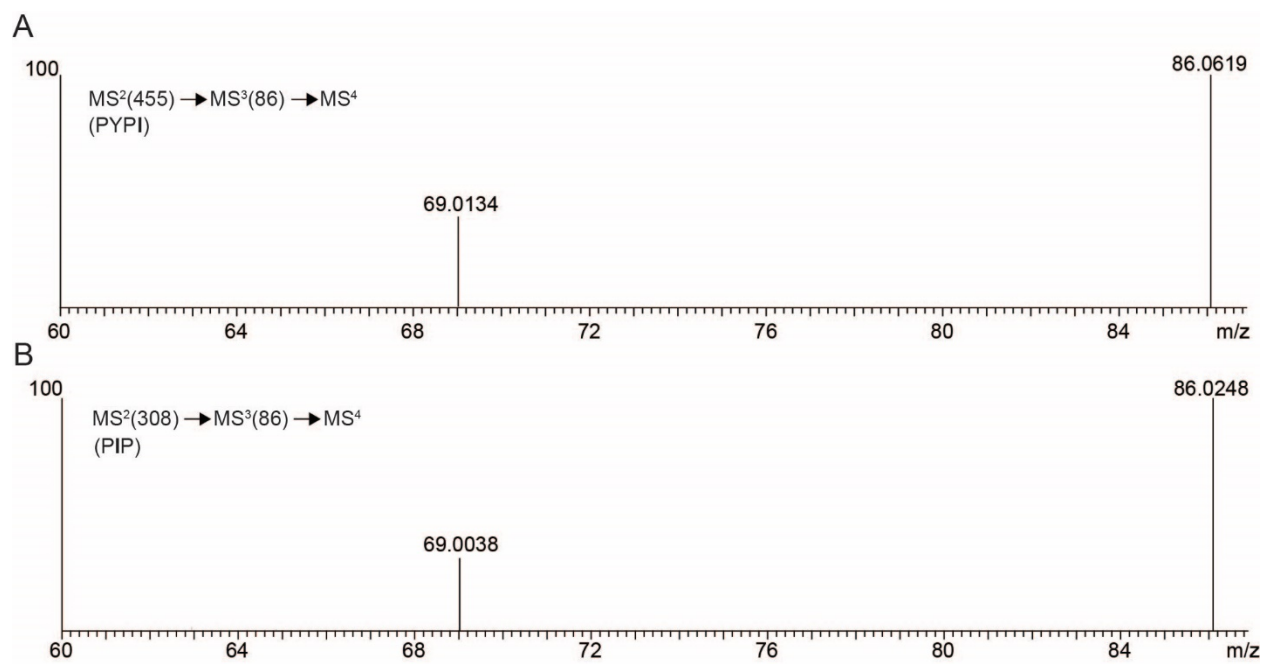**Fig. S22**: MS^2 sequencing of PRMP phakellistatin 18 cyclo(YPIFPIP).

Fig. S23: (**A**) MS^2(455)$\rightarrow MS^3$(86)$\rightarrow MS^4$ (**B**) MS^2(308)$\rightarrow MS^3$(86)$\rightarrow MS^4$ spectra for cyclo(YPIFPIP).
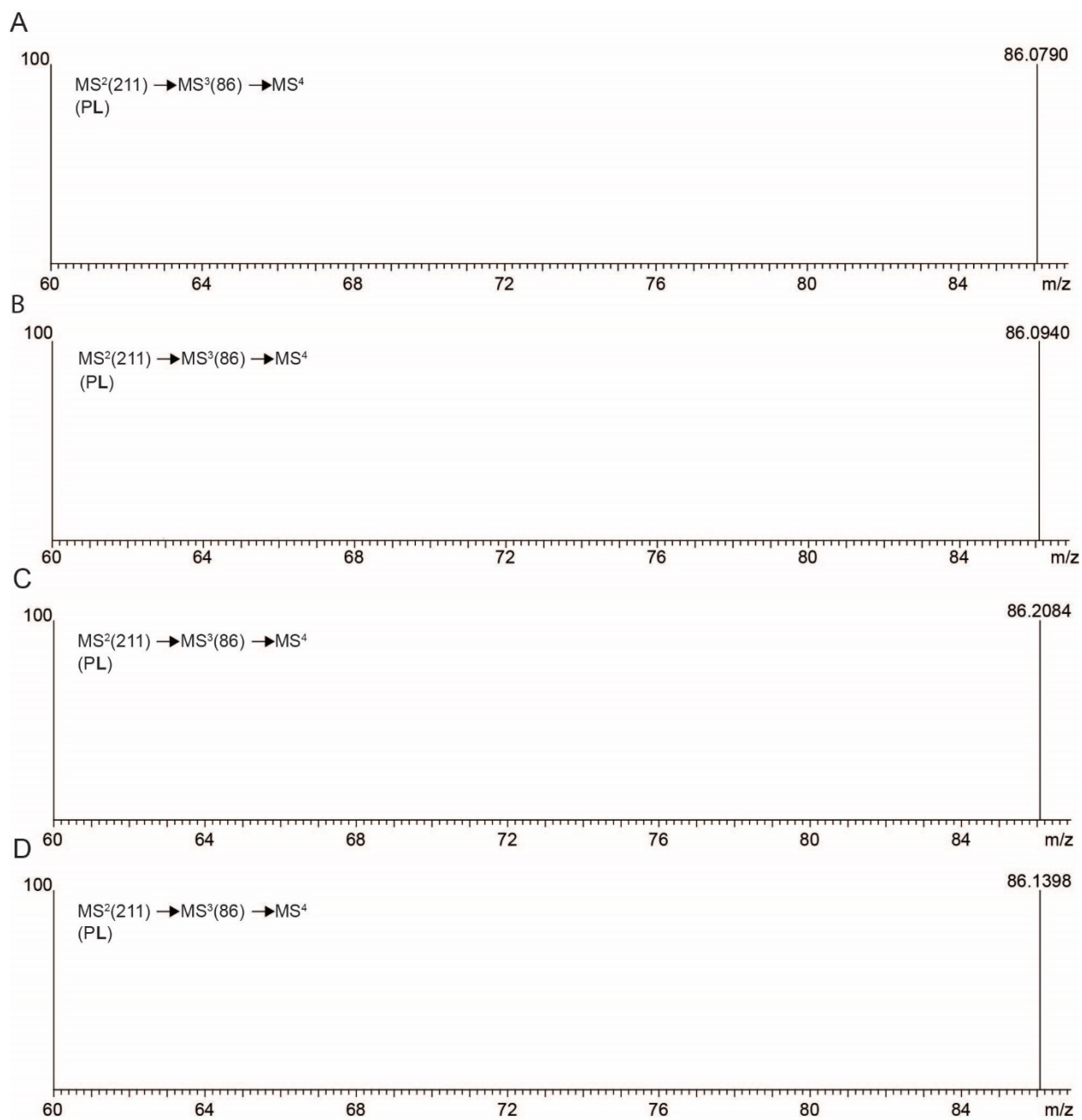
Fig. S24: $MS^2(211) \rightarrow MS^3(86) \rightarrow MS^4$ spectra for (**A**) cyclo(**L**PHPY**LL**GP), (**B**) cyclo(**L**PHPY**LI**GP), (**C**) cyclo(**L**PHPY**IL**GP), and (**D**) cyclo(**L**PHPY**II**GP).
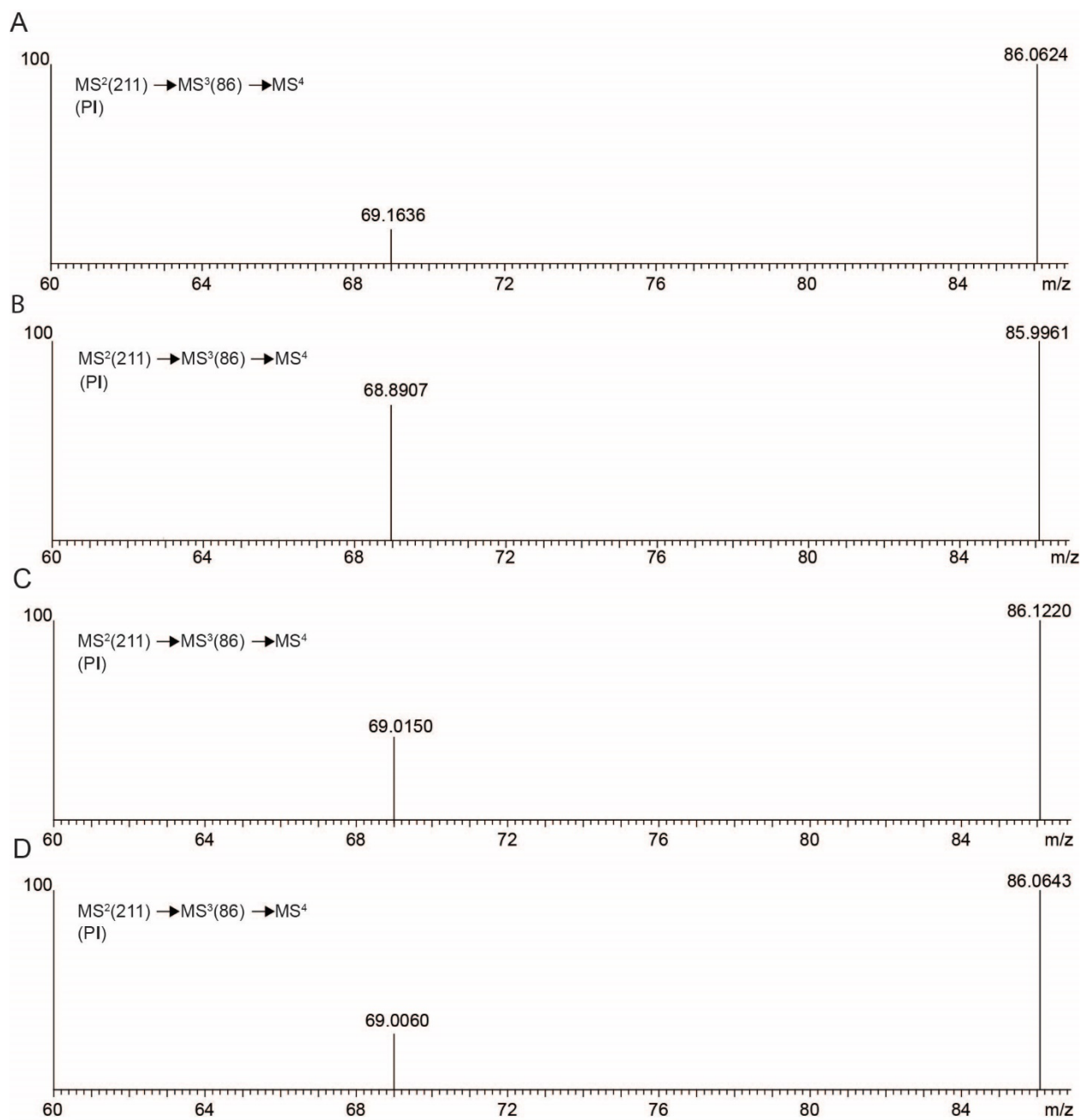
Fig. S25: $MS^2(211){\to}MS^3(86){\to}MS^4$ spectra for (**A**) cyclo(**IPHPYLLGP**), (**B**) cyclo(**IPHPYLIGP**), (**C**) cyclo(**IPHPYILGP**), and (**D**) cyclo(**IPHPYIIGP**).
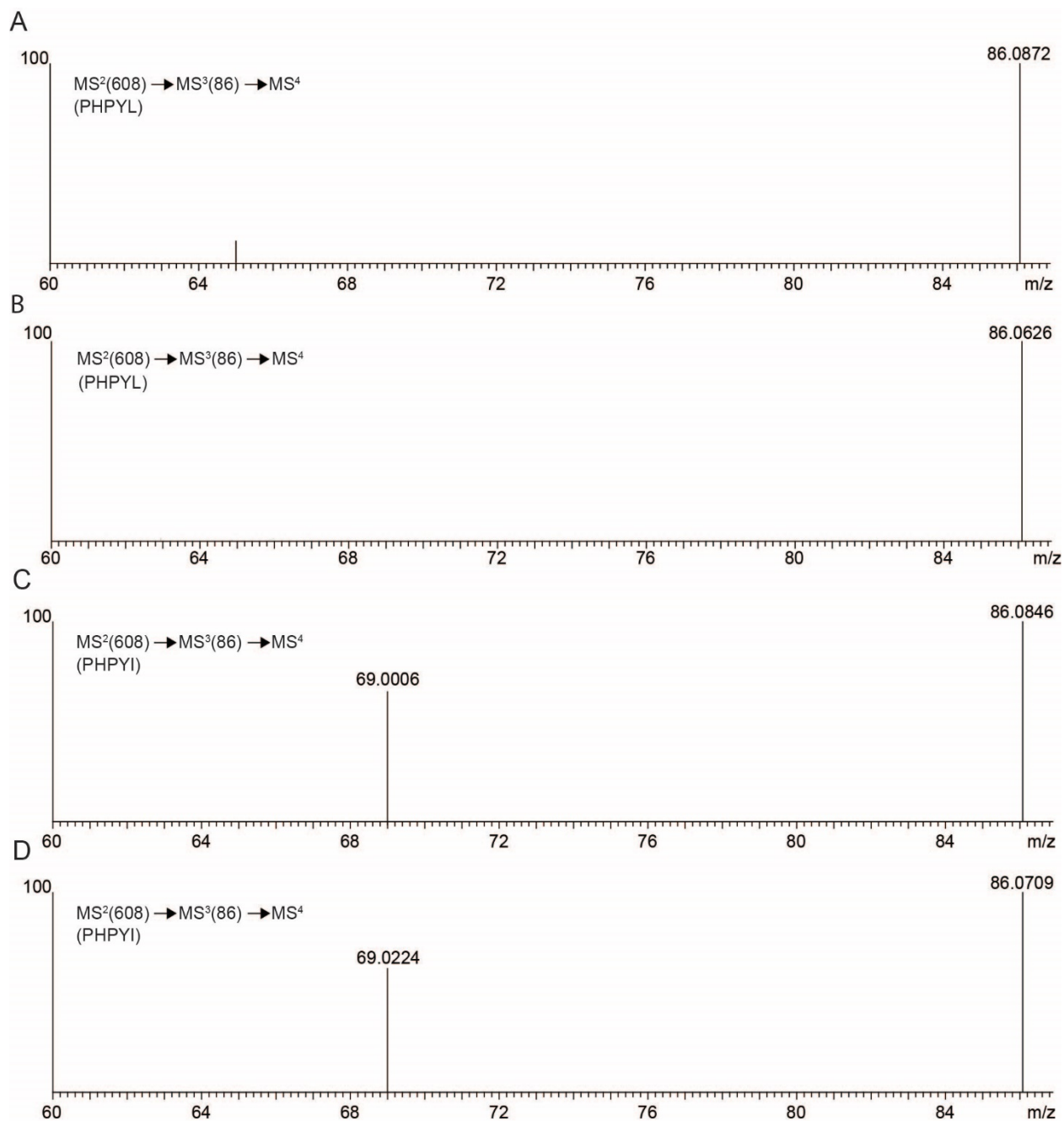
Fig. S26: (**A**) $MS^2(608) \rightarrow MS^3(86) \rightarrow MS^4$ spectra for (**A**) cyclo(**I**PHPY**LL**GP), (**B**) cyclo(**I**PHPY**LI**GP), (**C**) cyclo(**I**PHPY**IL**GP), and (**D**) cyclo(**I**PHPY**II**GP).

SUPPLEMENTARY REFERENCES

[1]   H. Ludewig, C. M. Czekster, E. Oueis, E. S. Munday, M. Arshad, S. A. Synowsky, A. F. Bent, J. H. Naismith, *ACS Chemical Biology* **2018**, *13*, 801-811.

[2]   aI. Mohanty, S. Podell, J. S. Biggs, N. Garg, E. E. Allen, V. Agarwal, *Mar. Drugs* **2020**, *18*, 124; bI. Mohanty, S. G. Moore, D. Yi, J. S. Biggs, D. A. Gaul, N. Garg, V. Agarwal, *ACS Chemical Biology* **2020**, *15*, 2185-2194.

[3]   B. J. Callahan, P. J. McMurdie, M. J. Rosen, A. W. Han, A. J. A. Johnson, S. P. Holmes, *Nature Methods* **2016**, *13*, 581-583.

[4]   E. Bolyen, J. R. Rideout, M. R. Dillon, N. A. Bokulich, C. C. Abnet, G. A. Al-Ghalith, H. Alexander, E. J. Alm, M. Arumugam, F. Asnicar, Y. Bai, J. E. Bisanz, K. Bittinger, A. Brejnrod, C. J. Brislawn, C. T. Brown, B. J. Callahan, A. M. Caraballo-Rodríguez, J. Chase, E. K. Cope, R. Da Silva, C. Diener, P. C. Dorrestein, G. M. Douglas, D. M. Durall, C. Duvallet, C. F. Edwardson, M. Ernst, M. Estaki, J. Fouquier, J. M. Gauglitz, S. M. Gibbons, D. L. Gibson, A. Gonzalez, K. Gorlick, J. Guo, B. Hillmann, S. Holmes, H. Holste, C. Huttenhower, G. A. Huttley, S. Janssen, A. K. Jarmusch, L. Jiang, B. D. Kaehler, K. B. Kang, C. R. Keefe, P. Keim, S. T. Kelley, D. Knights, I. Koester, T. Kosciolek, J. Kreps, M. G. I. Langille, J. Lee, R. Ley, Y.-X. Liu, E. Loftfield, C. Lozupone, M. Maher, C. Marotz, B. D. Martin, D. McDonald, L. J. McIver, A. V. Melnik, J. L. Metcalf, S. C. Morgan, J. T. Morton, A. T. Naimey, J. A. Navas-Molina, L. F. Nothias, S. B. Orchanian, T. Pearson, S. L. Peoples, D. Petras, M. L. Preuss, E. Pruesse, L. B. Rasmussen, A. Rivers, M. S. Robeson, P. Rosenthal, N. Segata, M. Shaffer, A. Shiffer, R. Sinha, S. J. Song, J. R. Spear, A. D. Swafford, L. R. Thompson, P. J. Torres, P. Trinh, A. Tripathi, P. J. Turnbaugh, S. Ul-Hasan, J. J. J. van der Hooft, F. Vargas, Y. Vázquez-Baeza, E. Vogtmann, M. von Hippel, W. Walters, et al., *Nature Biotechnology* **2019**, *37*, 852-857.